Available online at www.sciencedirect.com
ScienceDirect
Journal of Sound and Vibration 297 (2006) 627–634
JOURNAL OF SOUND AND VIBRATION
www.elsevier.com/locate/jsvi

Numerical study of self-adaptive vibration suppression for flexible structure using interior inlay viscous fluid unit method

Xiongwen Zhang[a], Jun Li[a], Hui Xu[b], Guojun Li[a,*]

[a]School of Power & Energy Engineering, Xi'an Jiaotong University, Xi'an, China
[b]School of Aerospace, Xi'an Jiaotong University, Xi'an, China

Received 8 September 2005; received in revised form 29 March 2006; accepted 10 April 2006
Available online 11 July 2006

Abstract

This paper investigates the usage of an interior inlay viscous fluid unit as a new vibration suppression method for flexible structures via numerical simulations. The first and second modes of vibration for a beam have been calculated using the commercial computational fluid dynamic package Fluent6.1, together with the liquid surface distribution and the fluid force. The calculated results show that the inlay fluid unit has suppressive effects on flexible structures. The liquid converges self-adaptively to locations of larger vibrations. The fluid force varies with the beam vibration at a phase difference of more than 180°. Thus the fluid force suppresses the beam vibration at most of the time.

1. Introduction

The residual vibration is one of the important features for flexible structures, and needs to be controlled precisely, quickly and reposefully. In order to suppress the residual vibration of flexible structures various suppression techniques have been proposed, for example, increasing the structure damping, improving the structure rigidity, or developing a complex control system. As a passive-control based technology, a new method using the interior inlay viscous fluid unit (IVFU) is different from the others. The IVFU is imbedded in the flexible structure, and the flexible structure is a compound configuration of both solid structures and a fluid unit. The instability of solid structures induces the fluid vibration and produces the Coriolis force and the centrifugal force in the fluid. Therefore, the fluid mass distribution in the solid cavity is not uniform. The fluid absorbs the energy from the solid structure and suppresses its vibration.

Present study investigates a quatrate IVFU beam as shown in Fig. 1. The filled viscous fluid could be water, silicon oil or other fluids. The effect of vibration suppression depends on the fluid used. The fluid fills just part of the interior cavity so that it can flow freely inside the cavity. In the present study, half of the cavity is filled by water and the other half by air. The fluid is trapped inside the cavity with a solid cover sealed by aluminum. Experiments with this configuration has been reported in Ref. [1] for an IVFU flexible structure beam with a

*Corresponding author. Tel.: +86 29 82668728; fax: +86 29 82665062.
E-mail address: liguojun@mail.xjtu.edu.cn (G. Li).

0022-460X/$ - see front matter © 2006 Elsevier Ltd. All rights reserved.
doi:10.1016/j.jsv.2006.04.014

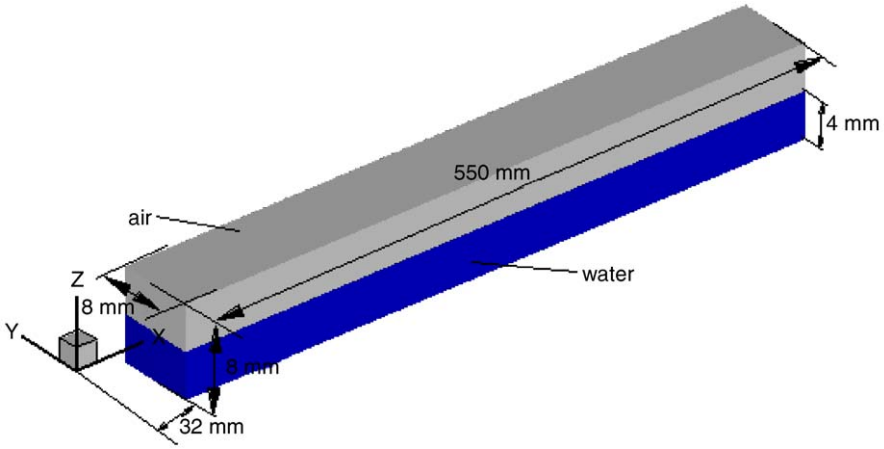

Fig. 1. Configurations of the IVFU beam used in experiments by Ref. [1].

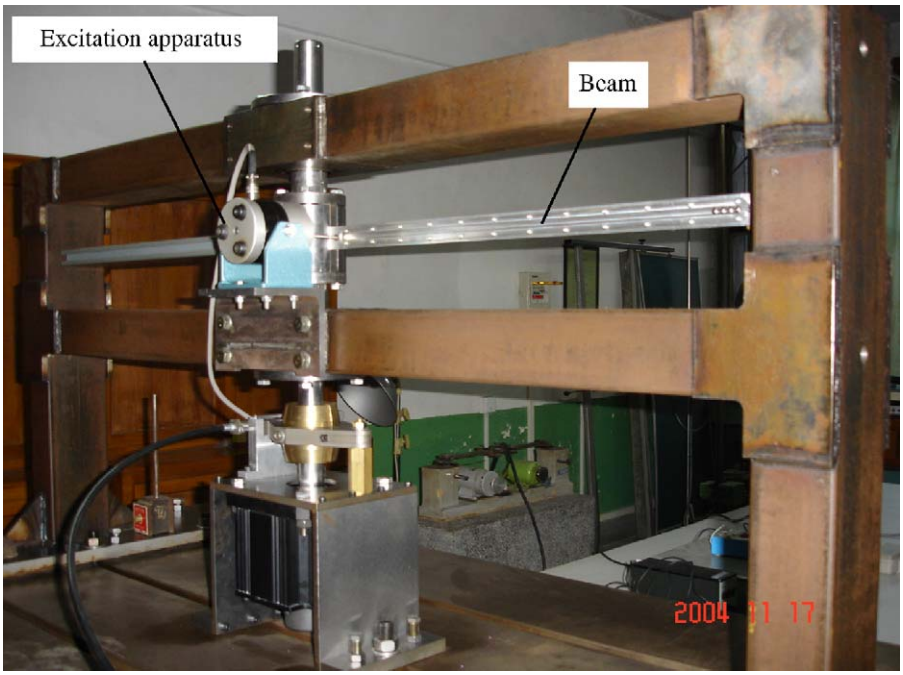

Fig. 2. The experimental setup for the IVFU beam.

stimulating aparatus vibrates the beam in the y direction. Fig. 2 shows the experiment setup. Due to the Coriolis force and the centrifugal force, the water moves inside the beam cavity. Experiments [1] showed that the beam vibration was reduced by 34.1% and 7.8% in the stimulation for the first and second vibration modes, respectively. Fig. 3 is the liquid surface distribution for both of the first mode and the second mode of vibration. The picture was taken by a digital camera (Sony DSC-P100).

This paper concentrates on using numerical method to investigate the interaction between the solid walls of the cavity and the fluid inside the IVFU. Numerical simulations have been carried out using the commercial computationl fluid dynamic package Fluent6.1. Results for the first and second vibration modes of main vibration type are presented together with the change in the water surface. Most importantly, the fluid vibration suppression mechanism has been analyzed via the fluid force.

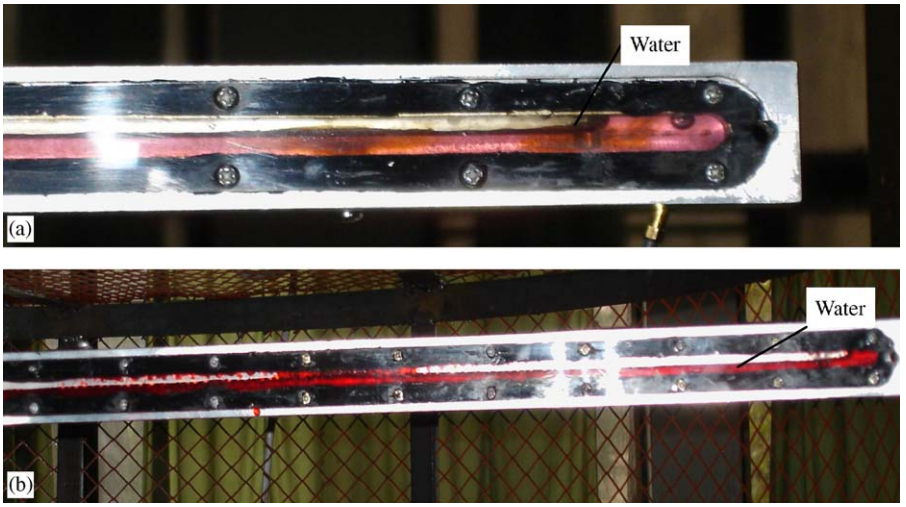

Fig. 3. The experimental results of water surface distribution for the IVFU beam: (a) the first vibration mode; (b) the second vibration mode.

2. Numerical method

2.1. Numerical model

Simulations in the paper are carried out for exactly the same IFVU model as used in Ref. [1]. As shown in Fig. 1, the cavity interior inlaying fluid of the quadrate cantilever beam has a dimension of $550 \times 8 \times 8$ mm. The lower half of its cavity is filled by water and the upper half by air. The operating pressure and temperature are 1.0135×10^5 Pa and 25 °C respectively. The cantilever beam is stimulated in the y direction for the first and second modes of principal mode. The excitation apparatus stimulate the beam in time as simple harmonics, given by:

$$W_1(x,t) = C_{y_1} Y_1(x) \sin(2\pi f_1 t) \quad \text{for the first mode,} \tag{1}$$

$$W_2(x,t) = C_{y_2} Y_2(x) \sin(2\pi f_2 t) \quad \text{for the second mode,} \tag{2}$$

where the frequencies f_1 and f_2 are chosen to be 22 Hz and 139 Hz, respectively. The coefficients C_{y1} and C_{y2} are set to 3.687e−4 and 6.245e−4. Fig. 4 shows the amplitudes of the cantilever beam response vibration along the x direction. And the principal modes of the cantilever beam equations are given by [2,3]:

$$Y_1(x) = \operatorname{ch}\beta_1 x - \cos\beta_1 x - 0.7341(\operatorname{sh}\beta_1 x - \sin\beta_1 x) \quad \text{for the first mode,} \tag{3}$$

$$Y_2(x) = \operatorname{ch}\beta_2 x - \cos\beta_2 x - 1.0184673(\operatorname{sh}\beta_2 x - \sin\beta_2 x) \quad \text{for the second mode,} \tag{4}$$

where $\beta_1 = 1.875/l = -3.1252$ and $\beta_2 = 4.694/l = -7.8235$ are constants.

2.2. Governing equations

Considering the vibration boundary condition, the two equations k–ε turbulent model is employed in the simulation. There two phases in the closed IVFU: air in the upper half and water in the lower half for the current configuration. The multiphase volume of fluid (VOF) model is assumed. In the control volume, volume fraction is calculated for each phase. All of the volume fractions sum to 1. For the qth phase, the

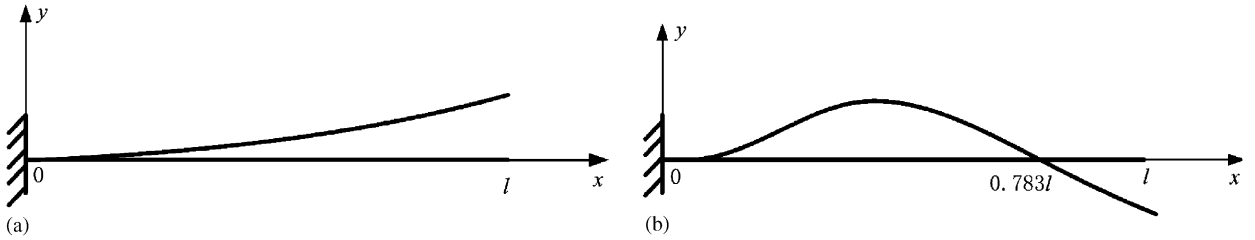

Fig. 4. The sketch figure of the beam principal modes: (a) the first mode; (b) the second mode.

volume fraction equation has the following form [7]:

$$\frac{\partial \alpha_q}{\partial t} + \boldsymbol{v} \cdot \nabla \alpha_q = 0, \tag{5}$$

with $\sum_{q=1}^{n} \alpha_q = 1$. For current study, n equal to 2.

The quantities in the transport equation are determined by the percentage of each phase volume fraction in the control volume. If we denote the two phases by subscripts 1 and 2 for water and air, respectively, for the current two-phase system, then the properties can be expressed as follows:

$$\phi = \alpha_1 \phi_1 + \alpha_2 \phi_2. \tag{6}$$

The shape of calculation domain changes in time due to the moving boundaries. Therefore, dynamic meshing is used for all simulations. In the arbitrary Lagrange–Euler (ALE) frame system, the general conservation equations for the incompressible fluid have the following form:

$$\frac{\partial \phi}{\partial t} + \nabla \cdot (\mathbf{u} - \mathbf{u}_m)\mathbf{u} = \frac{1}{\rho} \nabla \cdot (\Gamma \nabla \phi) + \frac{S_\phi}{\rho}, \tag{7}$$

where $\phi = 1$ stands for the mass conservation equation, $\phi = \mathbf{u}$ for the momentum equations and $\boldsymbol{\phi} = \boldsymbol{k}$ and $\boldsymbol{\varepsilon}$ for the turbulent kinetic energy and dissipation equations. $\mathbf{u}_m$ is the mesh moving velocity. The other parameters can be found in Refs. [4–7]. The mesh node coordinates are updated in time using Fluent's UDF interface.

In the unsteady iteration, the time step of 5.0e−5 s is used for the first mode vibration and 5.0e−6 s for the second mode vibration. Control volume method and the second order upwind difference scheme are used in the calculation. The SIMPLEC arithmetic is used in the pressure-velocity coupling iteration.

3. Results

Current study concentrates on the deformation of the water surface and the dynamic force. Results for time instants listed in Table 1 are of particular interests. At t_1 and t_9, the vibration of the beam arrives its negative peak and the solid wall is at zero vibration speed, at t_3 and t_7 the vibration amplitude is zero and the speed of vibration is at its maximum, and at t_5, the vibration amplitude is at its positive maximum.

Fig. 5 shows the distribution of the water surface for a case excited by the first mode. The vectors in Fig. 5 represent the solid wall vibration velocity. As show in Fig. 5(a,b), the wall vibration velocity is zero at the time t_1. At this time instant, the water surface is much flatter in the x direction than at time t_3. The water accumulates to the end of beam where the vibration amplitude is larger; see Fig. 5(c,d). This is very useful to reduce the beam vibration. In the y direction, the fluid moves in the opposite direction to the wall motion due to its inertia. For the case excited by the first mode, there is only one peak in the water surface.

Fig. 6 shows the water surface distribution results for the case excited by the second mode. It is different from the previous case where first vibration mode is applied. There are two peaks in the water surface in the x direction, appearing in the middle and at the end of the beam, where large vibration amplitudes are seen. This result is in agreement with the conclusion obtained from the case under first mode excitation. In other words, the large vibration amplitude accumulates more fluid. Comparing with Fig. 3 shows the simulation results for the water surface distribution is consistent with the experimental results of Ref. [1].

Table 1
Time sample instants

	t_1	t_2	t_3	t_4	t_5	t_6	t_7	t_8	t_9
First mode	$3T_1/4$	$7T_1/8$	T_1	$9T_1/8$	$5T_1/4$	$11T_1/8$			
Second mode	$3T_2/4$	$7T_2/8$	T_2	$9T_2/8$	$5T_2/4$	$11T_2/8$	$3T_2/2$	$13T_2/8$	$7T_2/4$

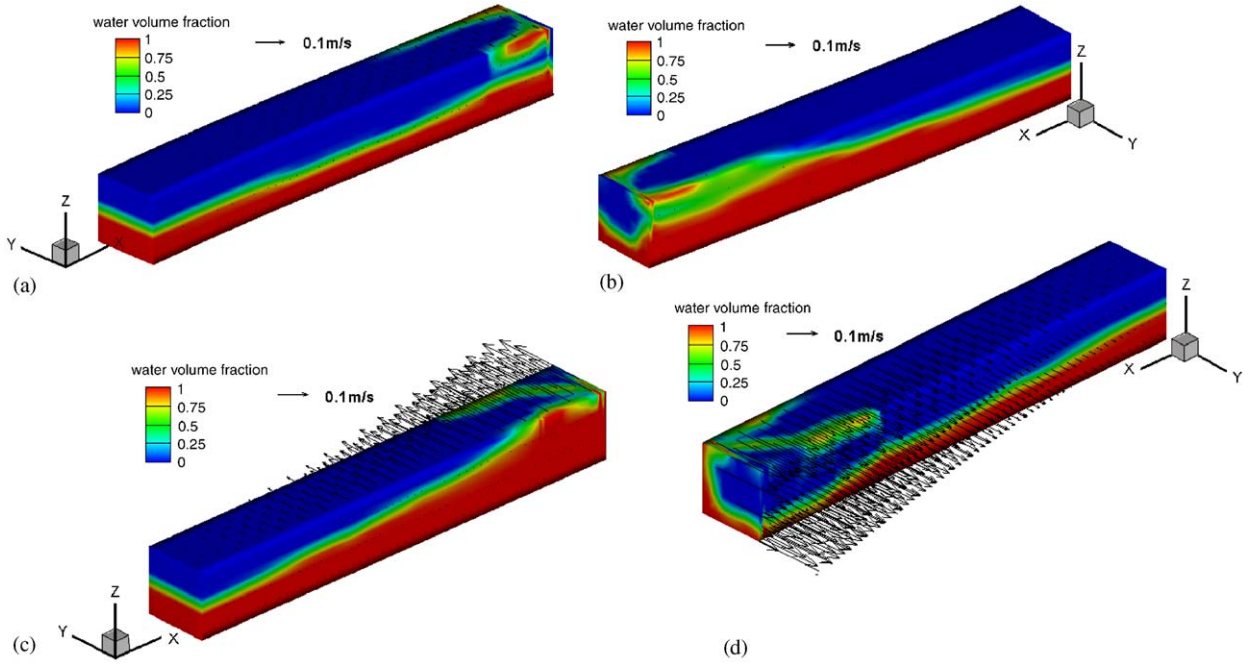

Fig. 5. The water surface distribution for the first mode case: (a) the backward for $t = t_1$; (b) the forward for $t = t_1$; (c) the backward for $t = t_3$; (d) the forward for $t = t_3$.

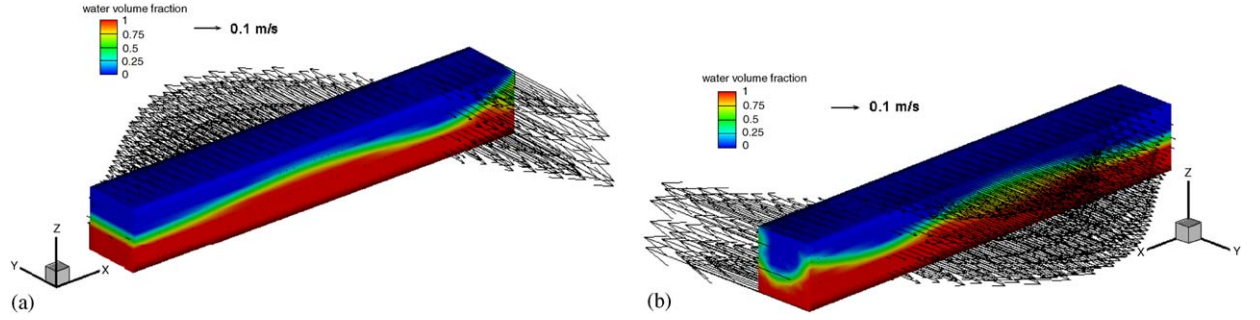

Fig. 6. The water surface distribution for the second mode case: (a) the backward for $t = t_3$; (b) the forward for $t = t_3$.

In order to calculate the force between the fluid and the solid wall, we divide the beam into 50 equal length segments in the x direction. The viscous force direction of the fluid is in the x direction. However, the main effective force to the beam vibration is in the y direction. Therefore, the viscous force can be neglected and only the pressure is considered in the calculation of the force for the y direction. For the solid wall on each

beam segment, the force is obtained by the following formula:

$$\mathbf{F}_i = \sum_k A_k p_k \cdot \mathbf{n}_k, \tag{8}$$

Where **F** is the force vector, A the area, p the pressure and **n** the normal vector. The subscript i and k is the index of segment and grid cell, respectively. Fig. 7 plots against time the vibration displacement and the force in the y direction for the segment, which the average radius is 0.5765 m for the first mode case and 0.2795 m for the second mode case. Data are plotted for segments located at the maximum displacement of the beam for

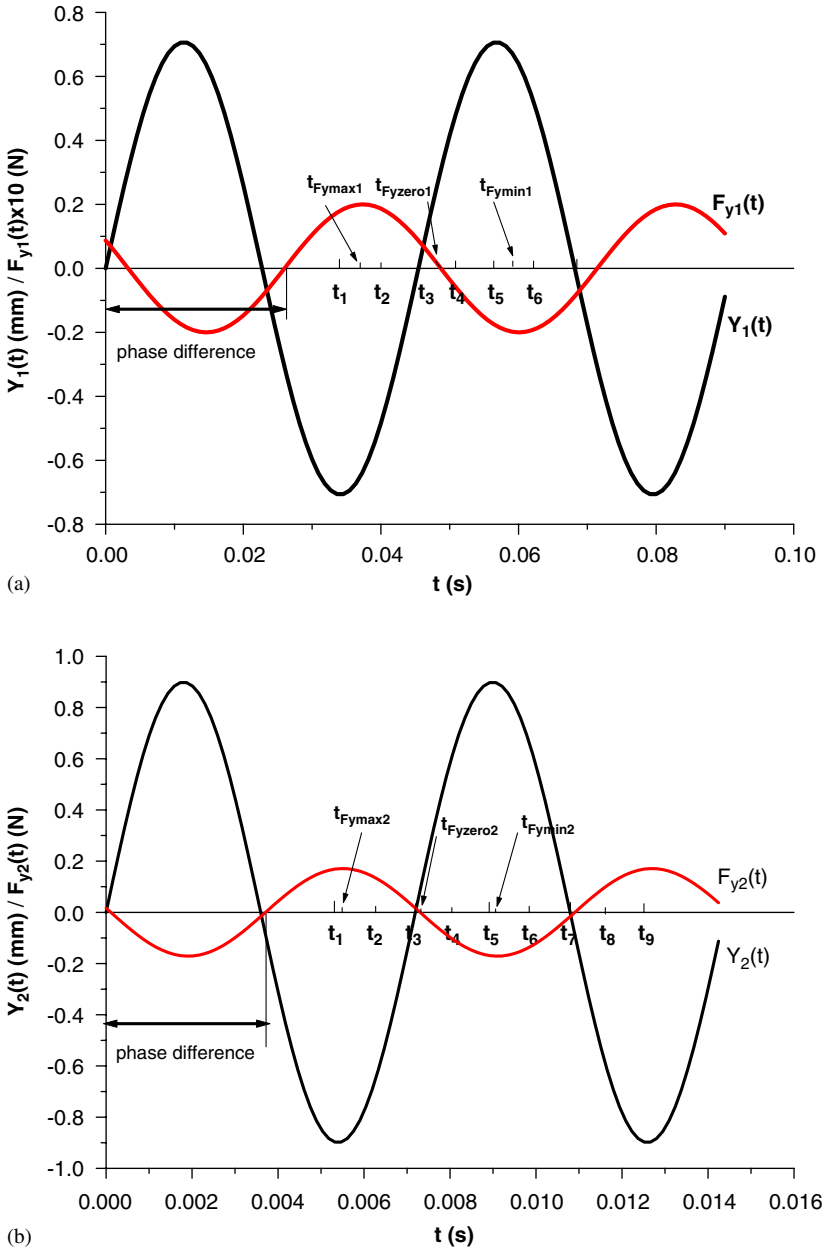

Fig. 7. The vibration of the displacement and the y-axial direction force for the beam: (a) the first mode (the segment average radius = 0.5765 m); (b) the second mode (the segment average radius = 0.2795 m).

both cases. As shown by Fig. 7, the direction of the force is opposite to the displacement direction for most of the time, during which the fluid force reduces the beam vibration. However, there are also time durations when the fluid force is in the same direction as the displacement, during which the fluid enhances the beam vibration. The phase difference between the fluid force and the bean displacement is 206° for the first mode case and 186° for the second mode case. As the vibration amplitude increases with the time, the fluid counterforce also increases.

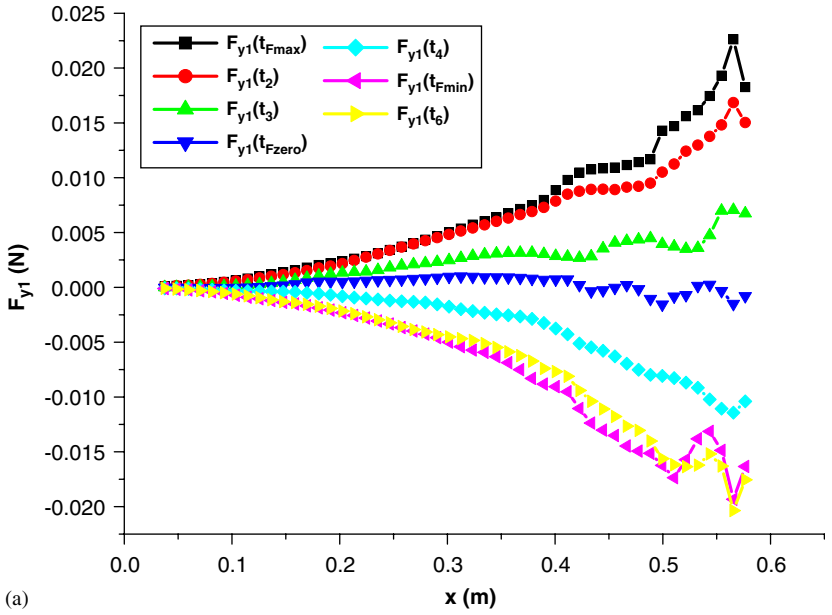

(a)

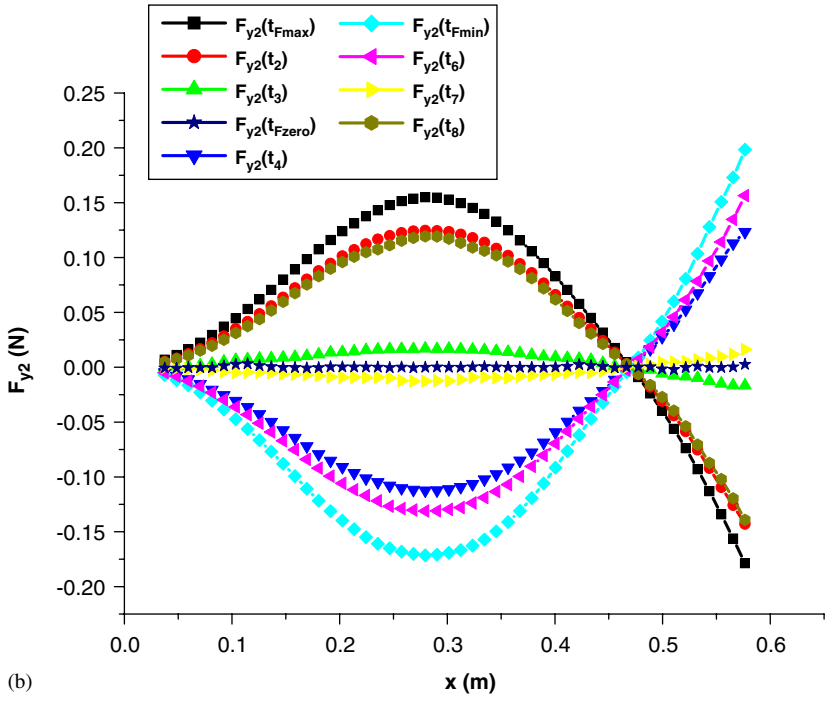

(b)

Fig. 8. The distribution of the force for y-axial direction on the beam: (a) the first mode; (b) the second mode.

Fig. 8 shows the distribution of the fluid force in the y direction along the beam. As shown in Fig. 8, the force varies periodically with time. There is only one peak for the first mode case. However, for the second mode case, there are two peaks, and the force direction is counter with the direction of beam displacement. This also shows that the counterforce of fluid is proportional to the vibration displacement. In Fig. 8(b), there exists a zero-force point at all the time, which locates at $x = 0.4557$ m, and its position is independent of time. Thus the vibration amplitude at this site is always equal zero.

4. Conclusion

The vibration suppression effect of an interior inlay fluid unit to flexible structures has been studied numerically. Simulations have been carried out for cases excited by the first and the second mode of the main vibration type. The unit is filled with water to half of its volume. Results for the liquid surface deformation and the fluid force are presented and analyzed.

Qualitatively, calculated results agree with the experiment carried out by Xu [1]. Analysis of the fluid force explained the vibration reduction mechanism of IVFU to the beam vibration. Water inside the IVFU converges to places where large vibration exists. For the first mode vibration, there is only one peak in the fluid surface, in contrast to two peaks for the second mode vibration. The period of fluid force is equal to that of the vibration displacement but, more importantly, with a phase difference. The phase difference between the force and the displacement is 206° for the first mode case, and has a smaller value of 186° for the second mode case. Due to the phase difference, the fluid force plays a suppressive role on the beam vibration during most of time. Moreover, the larger the vibration amplitude, the stronger the suppressive effect the IVFU applies to the flexible structure.

Acknowledgement

This study is financially supported by National Nature Science Foundation of China (NSFC 10372076).

References

[1] H. Xu, Theoretical and experimental study on self-adaptive vibration suppression for flexible structure using interior inlay viscous fluid unit method, Annual Report of NSFC, 2004.
[2] R.E.D. Bishop, D.C. Johnson, *The Mechanics of Vibration [M]*, Cambridge University Press, Cambridge, 1979.
[3] W.T. Thomson, *Theory of Vibration with Applications [M]*, Prentice-Hall, Inc., New York, 1972.
[4] E. Longatte, Application of Arbitrary Lagrange–Euler formulations to flow-induced vibration problems, *Journal of Pressure Vessel Technology* 125 (2003) 411–417.
[5] K. Yamamoto, Structural oscillation control using tuned liquid damper, *Computer and Structures* 71 (1999) 435–446.
[6] Y. Sugiyama, T. Katayama, E. Kanki, K. Nishino, B. Akesson, Stabilization of Cantilevered Flexible Structures by means of Internal Flowing Fluid, *Journal of Fluids and Structures* 10 (1996) 653–661.
[7] *Fluent User's Guide, Version 6.1*. Fluent Inc., Lebanon, NH, 2003.